RAFFLES BULLETIN OF ZOOLOGY **71**: 92–105
Date of publication: 14 February 2023
DOI: 10.26107/RBZ-2023-0008
http://zoobank.org/urn:lsid:zoobank.org:pub:2401E361-EBC2-44A2-B4DB-9F354680A5BB

Phylogeny and morphology of Himerometroidea (Echinodermata: Crinoidea) feather stars in Singapore

Shawne **Goh**[1,2], Randolph Z. B. **Quek**[2,3], Sze Hui **Foo**[2], Teresa Stephanie **Tay**[4], Charles G. **Messing**[5] & Danwei **Huang**[1,2,4*]

Abstract. Evaluating the diversity of crinoids (Echinodermata: Crinoidea) in Singapore accurately has been challenging due in part to inadequacies in crinoid taxonomy. Most species descriptions have neither incorporated morphological variation of juveniles into diagnostic characters nor analysed species' molecular phylogenetic affinities. In this study, we performed detailed morphological examination and phylogenetic analyses of the mitochondrial cytochrome c oxidase subunit I marker on Himerometroidea crinoids collected from the Singapore Strait, and showed that specimens could not be reliably identified to species based on existing taxonomic descriptions. Specifically, juveniles identified as *Heterometra* spp. and *Zygometra* sp., and adults as *H.* cf. *producta*, solely based on morphological features were revealed to comprise three distinct species: *Zygometra* cf. *comata*, *Heterometra schlegelii*, and *Dichrometra* sp. The juveniles were found to have sizes smaller than the ranges given in existing descriptions, with considerable variabilities in traits that limited the utility of morphology for species taxonomy. Features contributing to misidentification of specimens and their application in past species diagnoses are discussed. Revised descriptions of these species, as well as the recently revised *Homalometra crenulata*, are also presented. More broadly, this study emphasises the need to revisit diagnoses of crinoid species according to various ontogenetic stages and to uncover more congruent morphological characters based on a robust molecular phylogeny.

Key words. biodiversity, COI, integrative taxonomy, ontogenetic variation, phylogenetic analysis, tropical coastal habitats

INTRODUCTION

Crinoidea forms the earliest-branching class of extant Echinodermata (O'Hara et al., 2014). All extant crinoids are part of Articulata, the only remaining subclass after the Permian-Triassic extinction (Hess, 1999; Baumiller et al., 2010). Traditionally, taxonomic classification of crinoids has followed A. H. Clark's monographs based solely on morphological features (AH Clark, 1915, 1921, 1929, 1931, 1941, 1947, 1950; AH Clark & AM Clark, 1967). However, this is currently a subject of intense research as many of the supposed diagnostic features have been shown to display unexpected variation and phenotypic plasticity (Summers et al., 2014; Taylor et al., 2017), and some taxonomic descriptions were based on small sample sizes in specimen representation (Messing & Tay, 2016). Critically, ecophenotypic and ontogenetic variations of characters have not been considered in most taxonomic descriptions (Taylor, 2015).

With the increasing application of molecular approaches on crinoids, their taxonomic classification has been subjected to extensive revision (Hemery et al., 2013; Summers et al., 2014, 2017). For example, the superfamily Himerometroidea AH Clark, 1908c has been revised repeatedly at both family and genus levels (Owen et al., 2009; Hemery et al., 2013; Summers et al., 2014, 2017). In particular, Taylor (2015) showed Colobometridae, Zygometridae, Mariametridae, and Himerometridae to be polyphyletic. Taylor et al. (2017) reduced multiple species of *Himerometra* to synonyms and, in 2018, placed *Dichrometra*, *Lamprometra*, and *Liparometra* into a single *Dichrometra* genus (Taylor et al., 2018). Most recently, Foo et al. (2021) transferred *Heterometra crenulata* (Carpenter, 1882) into *Homalometra*, and *Ho. crenulata* is now regarded as the senior synonym of *Ho. denticulata*.

Of all the Himerometroidea taxa, *Heterometra* spp. are some of the hardest to distinguish as many diagnostic features such as cirri ornamentation, proximal pinnule ornamentation, and proportions of ossicles can overlap between genera and

Accepted by: Tan Koh Siang

[1]Lee Kong Chian Natural History Museum, National University of Singapore, 2 Conservatory Drive, Singapore 117377, Singapore; Email: huangdanwei@nus.edu.sg (*corresponding author)

[2]Department of Biological Sciences, National University of Singapore, 16 Science Drive 4, Singapore 117558, Singapore

[3]Yale-NUS College, National University of Singapore, 16 College Avenue West, Singapore 138527, Singapore

[4]Tropical Marine Science Institute, National University of Singapore, 18 Kent Ridge Road, Singapore 119227, Singapore

[5]Halmos College of Natural Sciences and Oceanography, Nova Southeastern University, 8000 N Ocean Drive, Dania Beach, FL 33004, United States of America

ISSN 2345-7600 (electronic) | ISSN 0217-2445 (print)

species. For example, the proximal pinnules of *He. amboinae* (AH Clark, 1912) and *He. singularis* AH Clark, 1909b, are both smooth and have keeled proximal pinnulars, yet these traits are considered diagnostic characters for both species (Hess & Messing, 2011; Messing & Tay, 2016) (AH Clark used both 'carination' and 'keel' to refer to the carinate extensions of pinnulars; for consistency, we use 'carination' and 'carinate extension' here). AH Clark (1941) also noted the problematic nature of the diagnosis of *He. producta*, as "some forms of *H. crenulata* approach *H. producta* which may possibly turn out to be merely an extreme variation of it while *H. producta* and *H. propinqua* [AH Clark, 1912] probably will be found to intergrade" (AH Clark, 1941: 226). He noted the close resemblance of *He. producta* with *He. proquinqua* and *Ho. crenulata*, differing only in the slenderness of the cirri (AH Clark, 1941: 277–278), a vague character far from useful in species diagnosis, as well as the number of cirri and pinnule segments (AH Clark, 1941: 277), which are known to vary within species (Messing & Tay, 2016). Adding to the complexities of *Heterometra* identification, juveniles are typically underrepresented or unexamined in these studies. They are known to be notoriously difficult to identify due to their small size, premature development of diagnostic characters, as well as insufficient collection. For example, due to uncertainty in the species identities of juveniles, Messing & Tay (2016) excluded those specimens from their assessment of extant crinoids in Singapore.

Notably, there has been no study on the identity of juvenile crinoids in Singapore, which is home to 14 nominal species from Himerometroidea (Messing & Tay, 2016). Local diversity is confounded by the above taxonomic uncertainties, translating to potentially inaccurate richness estimates at species, genus, and family levels (Messing & Tay, 2016; Summers et al., 2017; Taylor et al., 2018). Therefore, this study aims to determine the species identities of Himerometroidea feather stars based on a phylogenetic analysis of mitochondrial cytochrome c oxidase subunit I (COI) sequences, evaluate existing taxonomic descriptions with an emphasis on juveniles, and update the species descriptions with characteristics evaluated in the context of the molecular phylogeny and morphology of juvenile specimens.

MATERIAL AND METHODS

Specimen collection. A total of 11 Himerometroidea juveniles and seven adult specimens preliminarily identified as *Heterometra* cf. *producta* were examined in this study. These specimens were collected using a rectangular dredge or beam trawl during the Comprehensive Marine Biodiversity Survey (CMBS) from May to June 2013 (Tan et al., 2016) at eight sampling stations (1°10.125′N, 103°45.419′E, Raffles Lighthouse; 1°12.416′N, 103°49.858′E, Sister's Island; 1°12.024′N, 103°50.170′E, Outside Eastern Boarding Ground; 1°12.202′N, 103°52.178′E, Next to Boarding Ground A, 1°13.036′N, 103°52.820′E, Singapore Port Limit; 1°13.537′N, 103°53.793′E, Outside Eastern Boarding Ground; 1°17.838′N, 104°04.157′E, Eastern Bunkering A; 1°18.140′N, 104°04.22′E, Eastern Bunkering A) between depths of 135 m and 22 m in the Singapore Strait. Their juvenile status was determined by the length of their longest arm (≤ 4 cm) and the diameter of their centrodorsal (≤ 2 mm). Due to the premature state of the juvenile specimens, none of them were identified confidently to species level—two specimens were presented as *Ho.* cf. *crenulata*, while the other eight and one specimen were identified only to genus level as *Heterometra* sp. and *Zygometra* sp., respectively. All specimens were preserved in 70% or 100% ethanol and deposited at the Zoological Reference Collection, Lee Kong Chian Natural History Museum, National University of Singapore.

Abbreviations of specimen repositories: EXEMS = Royal Albert Memorial Museum & Art Gallery (Exeter Museum), Exeter, UK; USNM = National Museum of Natural History, Washington, DC, USA; ZMC = Zoological Museum, Copenhagen, Denmark; ZMH = Zoologisches Museum für Hamburg, Hamburg, Germany; ZRC = Zoological Reference Collection, Lee Kong Chian Natural History Museum, Singapore.

Abbreviations of source institutions for sequenced material: FMNH = Florida Museum of Natural History, Gainesville, FL, USA; ME = Museum Victoria, Melbourne, VIC, Australia; MNHN = Muséum national d'Histoire naturelle, Paris, France; NSU = Crinoid collection, Nova Southeastern University, Dania Beach, FL, USA; NSMT = National Museum of Science and Technology, Tokyo, Japan; OMNH = Osaka Museum of Natural History, Osaka, Japan; SAM = South Australian Museum, Adelaide, SA, Australia; SIO-BIC = Benthic Invertebrate Collection, Scripps Institution of Oceanography, La Jolla, CA, USA.

Molecular phylogenetic analysis. Extraction of genomic DNA was conducted using the Qiagen DNeasy Blood and Tissue Kit. Polymerase chain reaction (PCR) of the COI marker was carried out using the primers mlCOIintF (forward; 5′-GGW ACW GGW TGA ACW GTW TAY CCY CC-3′) and HCO2198 (reverse; 5′-TAA ACT TCA GGG TGA CCA AAA AAT CA-3′) (Folmer et al., 1994) to amplify a 313-bp fragment of COI (Leray et al., 2013). Initial attempts had aimed to sequence a longer COI fragment of 1100-bp length using the primers CO1-F (5′-AGT CGT TGG TTG TTT TCT AC-3′) and CO1-R (5′-CAA TGA GTA AAA CCA GAA-3′) (Helgen & Rouse, 2006), but failed due to DNA degradation as verified by gel electrophoresis post-extraction. Reagents for PCR comprise 12.5 µL GoTag G2 Green Master Mix (Promega) or KAPA Hifi HotStart ReadyMix (Roche), 1.0 µL each of 10 µM forward and reverse primers, 1.0 µL DNA template, and 9.5 µL nuclease-free water. Reactions were performed with 3 minutes of initial denaturation at 94°C, followed by 35 cycles of 94°C for 45 seconds for denaturation, 48°C for 45 seconds for primer annealing and 72°C for 1 minute for extension, and ending with a final extension at 72°C for 3 minutes. PCR products were purified using SureClean Plus (Bioline) and cycle sequencing was performed with the BigDye® Terminator v3.1 Cycle

Sequencing Kit (Applied Biosystems). DNA precipitation was performed using PureSEQ (Aline Biosciences), and sequencing carried out on an ABI 3730XL Genetic Analyser (Applied Biosystems). Post-sequencing, quality check of chromatograms and sequence assembly were done on Geneious v11.1.5 (Kearse et al., 2012). Sequences were deposited in GenBank under accession numbers OP580101–OP580117.

Sequence data were aligned using MAFFT v7.475 (Katoh et al., 2002; Katoh & Standley, 2013), along with 137 Himerometroidea sequences from GenBank and past publications (see Foo et al., 2021). *Colobometra perspinosa* (KM491785) was designated as an outgroup. Pairwise uncorrected genetic distances were computed in Geneious v11.1.5 (Kearse et al., 2012). The COI sequence alignment was analysed under maximum likelihood (ML) with RAxML v8.2.12 (Stamatakis, 2006, 2014), under the GTRGAMMA model with 50 random starting trees. Node supports were assessed with bootstrapping using 1,000 pseudoreplicates. Bayesian inference (BI) was performed using MrBayes v3.2.7 (Huelsenbeck & Ronquist, 2001; Ronquist et al., 2012) under the GTR+I+G model, selected according to jModelTest v2.1.10 (Posada, 2008). Two Markov Chain Monte Carlo runs were performed with 12 million generations each, and sampling was done every 100th tree. Following burn-in of the first 20,001 trees, 100,000 trees were retained and summarised as a majority-rule consensus tree.

Morphological examination. Specimens were examined under a Leica M205C stereomicroscope and photographed with a Leica MC190 HD digital microscope camera. Initial species identification was performed independent of the molecular phylogenetic analysis. Characters examined included size of centrodorsal, number of arms, length of longest arm, number of cirri and cirrals, presence of beads on radials, number of ossicles in each division series, articulation between ossicles, as well as proximal pinnule and cirri ornamentation. Where syzygy in specimens was not clearly visible, the covering tissue was removed by adding 10% bleach. The type specimens of studied species were not examined; comparisons were made based on published descriptions. Morphological terminology followed Messing & Tay (2016) and Hess & Messing (2011). Traits marked with asterisk (*) in the description of *Ho. crenulata* were adapted from AH Clark (1941).

RESULTS

Molecular phylogenetic analysis. Of the 18 specimens studied, sequences were obtained successfully for 17 specimens (sequencing failed for SS-3643-7, ZRC.ECH.1976). As determined by their phylogenetic affinities based on COI, nearly all the identities of the specimens were incongruent with their original identification. Eight specimens initially identified as *Heterometra* cf. *producta* (n = 4), *Homalometra* cf. *crenulata* (n = 1) and *Heterometra* sp. (n = 3) were determined to be *He. schlegelii* (AH Clark, 1908b). These specimens were placed in the same clade as 32 other local *He. schlegelii* sequences and *He. savignii* (Müller, 1841) (ML bootstrap value = 98; Bayesian posterior probability = 0.99), which together were sister to *He. quinduplicava* (Carpenter, 1888) and *He. sarae* AH Clark, 1941 with strong support from ML bootstrap analysis (95) but low support from Bayesian posterior probability (0.56) (Fig. 1). Intraspecific genetic distances within *He. schlegelii* had a mean of 0.073% (range: 0–0.911%), while interspecific distances with *He. savignii* had a mean of 0.007% (range: 0–0.115%).

Seven specimens that were initially identified as *Heterometra* sp. (n = 5), *He.* cf. *producta* (n = 1), and *Ho.* cf. *crenulata* (n = 1) were revealed to be *Dichrometra* sp., as they were found nested within the *Dichrometra* clade with high ML bootstrap support (89) and Bayesian posterior probability (0.99). Intraspecific genetic distances within *Dichrometra* sp. had a mean of 0.104% (range: 0–0.400%).

The final two specimens initially identified as *He.* cf. *producta* and *Zygometra* sp. formed a monophyletic group with nine other local *Zygometra* cf. *comata* AH Clark, 1911 sequences and *Z. andromeda* AH Clark, 1912 (ME79). This was strongly supported by both ML analysis (bootstrap value = 100) and BI (posterior probability = 1). Intraspecific genetic distances within *Zygometra* cf. *comata* had a mean of 0.026% (range: 0–0.110%), while interspecific distances with *Z. andromeda* had a mean of 1.066% (range: 0.676–1.292%).

Morphological examination. The smallest juveniles were generally smaller than the minimum sizes given in the literature, although there was overlap for the largest juveniles. The sizes of adult specimens mostly fell within the size ranges listed in existing literature, but some of the smaller adults were smaller than these ranges. Number of ossicles in each division series for both juveniles and adults were generally consistent with literature. Notably, *Zygometra* cf. *comata* juveniles and adult specimens have a smaller number of arms than that in literature, while the number of cirrals were within or even greater than the given range in previous taxonomic descriptions.

On qualitative traits, adult specimens were mostly consistent with literature in proximal pinnule ornamentation, relative size, and centrodorsal shape. With the exception of *Zygometra* cf. *comata*, morphological characters in juveniles vary within species and differ from literature, notably in cirri ornamentation and relative sizes of proximal pinnules. Taxonomic descriptions of these species given below have been revised to include juvenile features (AH Clark, 1941; Hess & Messing, 2011; Messing & Tay, 2016; Taylor et al., 2018).

The six specimens originally identified as *Heterometra* cf. *producta* were generally similar in size. While they differed in most morphological characters, the specimens shared distally flagellate proximal pinnules with pinnulars that were smooth with no projections, and cirri that bore triangular projections on middle cirrals and became progressively sharper to resemble spines in distal cirrals.

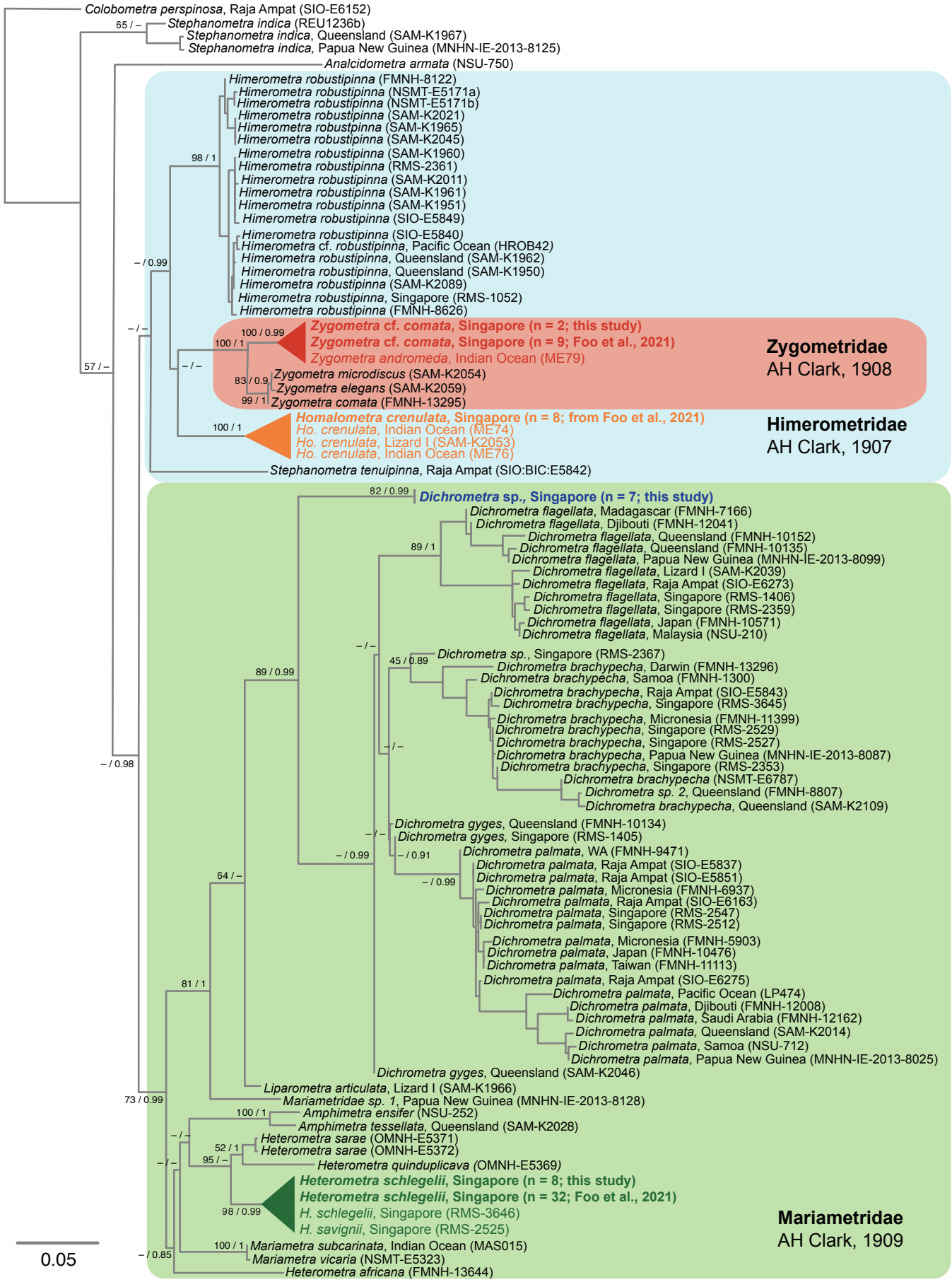

Fig. 1. Maximum likelihood (ML) reconstruction of superfamily Himerometroidea based on cytochrome c oxidase subunit I (COI) sequences. Number in parentheses indicates specimens within collapsed clades. Values at nodes species-level and above are shown as follows: ML bootstrap support values (≥ 50) / Bayesian posterior probability (≥ 0.8).

SYSTEMATICS

Order Comatulida, AH Clark, 1908c

Superfamily Himerometroidea AH Clark, 1908c

Family Himerometridae AH Clark, 1907

Genus *Homalometra* AH Clark, 1918

Homalometra crenulata (Carpenter, 1882)
(Fig. 2)

Antedon crenulate Carpenter, 1882: 507.
Antedon decipiens Bell, 1882: 534.
Antedon irregularis Bell, 1882: 534.
Antedon denticulata Carpenter, 1888: 130.
Antedon dubia Carpenter, 1888: 258.
Craspedometra aliena AH Clark, 1909c: 31.
Amphimetra crenulata AH Clark, 1913: 16.
Craspedometra aruensis Reichensperger, 1913: 99.
Heterometra crenulata AH Clark, 1918: 79.
Homalometra denticulata Foo et al., 2021: 638.

Holotype. EXEMS 263/1903/B/57 (fragments from specimen ZMH 487-526 [507] which is missing).

Material examined. Sta. SUB07, SE of St. John's Island, start 01°12.671′N, 103°51.232′E, end 01°12.607′N, 103°51.145′E, 53.7–34.8 m, 19 April 2016 (n = 1; TR0322, ZRC.ECH.1637); sta. SUB19, S of St. John's Island, start 01°12.533′N, 103°51.097′E, end 01°12.497′N, 103°51.120′E, 43.8–40.6 m, 2 June 2016 (n = 1; TR0951, ZRC.ECH.1679); sta. SUB21, SE of St. John's Island, start 01°12.519′N, 103°51.399′E, end 01°12.516′N, 103°51.486′E, 60.8–56.2 m, 2 June 2021 (n = 3; TR0952i, ZRC.ECH.1639; TR0952ii, ZRC.ECH.1636; TR0952iii, ZRC.ECH.1638); sta. SUB36, SW of St. John's Island, start 01°12.649′N, 103°50.659′E, end 01°12.617′N; 103°50.613′E, 40.6–38.3 m, 30 June 2016 (n = 2; TR2137, ZRC.ECH.1632; TR2144iii, ZRC.ECH.1628).

Diagnosis. A highly variable species. First three outer pinnules enlarged and are moderately to strongly prismatic. P_1 almost always the smallest, P_2 and P_3 equally likely to be the largest (where P_n denotes the n^{th} exterior pinnule from the base of each undivided arm). Proximal pinnulars of the proximal pinnules bear carination (Fig. 2A) but might be absent in juveniles (Fig. 2B). From the third or fourth pinnular onwards, their distal corners on the abambulacral side always ornamented with serrated triangular processes which may be conspicuous and broadly rounded (Fig. 2C) or small, compact, and in tight apposition to the pinnules (Fig. 2D). The distal margin of the distal pinnulars often bordered with minute spines that form a partial rim across the abambulacral surface, giving the distal edges of the pinnulars a serrated profile (Fig. 2E). Radials may be partially or completely concealed in the midradial lines. When exposed, the distal edges are most likely bordered with bead-like tubercles (Fig. 2F), though exceptions of smooth radials were seen in some specimens including in one juvenile.

Description. Centrodorsal discoidal to hemispherical, with the polar area either flat and barren* or appearing uneven with indentations which may resemble obsolete cirral sockets (Fig. 2G) (* = adapted from AH Clark, 1941). Cirri as little as XI* in small specimen and as many as XXXV* in adults (XVII–XXX in examined specimen), arranging marginally in two alternating rows (number of cirri denoted in Roman numerals). Number of cirrals range between 17 and 46* (usually 30–40). Cirral mostly broader than long or as broad as long except in the middle cirrals (~6–11) of some specimens. Middle to distal cirrals bear carinae with varying morphology which may be absent in immature specimens. In typical examples, the carinae project distally into a triangular extension (Fig. 2H) while in other cases, they are divided into 2–3 teeth (Fig. 2J). Note that different types of carinae could be present in the same individual on different cirri. The cirri of immature specimens may appear smooth, slender, and tapered to a point with the lack of carination, as seen in some of the western Australian specimens, including in the holotype of *Homalometra denticulata* (Carpenter, 1888), now a junior synonym. Opposing spine always present on the penultimate cirral. Brachitaxes up to three series, with IBr2 united by synarthry, IIBr either 2 or 4(3+4), and IIIBr chiefly absent or two ossicles when present, but IIIBr4(3+4)* has also been reported in some specimens examined by AH Clark (1941) (Roman numerals with "Br" and an Arabic numeral refer to a particular brachitaxis, e.g., IBr2 = primibrachial series comprising two ossicles; particular ossicles are identified with a lower-case "br" followed by an Arabic numeral, e.g., Ibr2 = second ossicle of the primibrachial series; plus sign denotes syzygy articulation between specific ossicles, e.g., IIBr4(3+4) = secondibrachial series comprising four ossicles with syzygy between ossicles IIbr3 and IIbr4). The first two segments beyond each axillary bear a weak synarthrial tubercle at the middle line of their junction. Proximal brachials discoidal. The following brachials triangular to wedge-shaped, with a variable tendency to overlap dorsally, and their broader ends project alternately on opposite sides of the arm to a greater or less extent*. The sides of the proximal brachials may be flattened or swollen. First syzygial pair on the undivided arms always between brachials 3+4, subsequent syzygial position variable. Articular tubercles present.

Remarks. Habitat generally with rocky substrate, coarse sand, broken shells, shelly mud, laterite rock and/or gravel. Depth range extends from shoreline to 111 m (60.8–34.8 m for the local specimens).

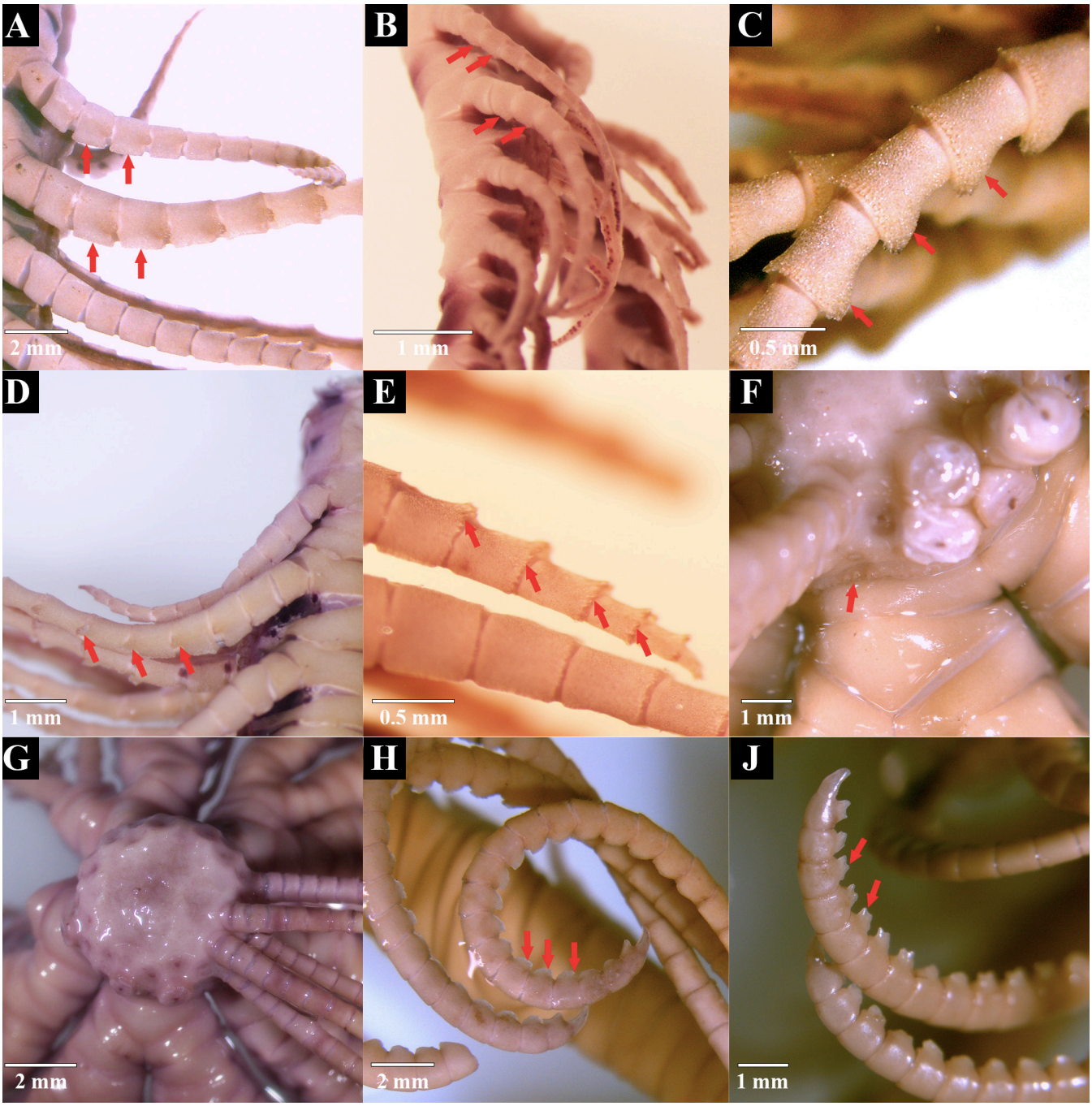

Fig. 2. *Homalometra crenulata* morphological characters. Red arrows indicate specific features described for each image (A–F, H–J). A, carination of proximal pinnulars of proximal pinnules; B, lack of carination on the proximal pinnulars of juvenile proximal pinnules; C, broad, round triangular processes on distal corners of ambulacral side of proximal pinnules; D, unique pinnular with triangular processes of proximal pinnulars are small, compact, and tightly appose to the pinnulars; E, serration on the distal margin of distal pinnulars; F, bead-like tubercles on the distal edge of a radial; G, polar area of centrodorsal bumpy and uneven, with indentations that resemble obsolete cirri sockets; H, cirrals with a distally-directed triangular carinate extension; J, aboral projections compressed laterally on distal cirrals, terminating in 2–3 weak or strong teeth, or almost a flattened tip (lower-right arrow).

Family Zygometridae AH Clark, 1908a

Genus *Zygometra* AH Clark, 1907

***Zygometra* cf. *comata* AH Clark, 1911**
(Fig. 3)

Zygometra comata AH Clark, 1911: 762.

Holotype. USNM 35137.

Material examined. Sta. DR125, Sister's Island, start 01°12.416′N, 103°49.858′E, end 01°12.433′N, 103°49.817′E, 30.8–25.3 m, 30 May 2013 (n = 1; SS-3643-6, ZRC.ECH.1975); sta. DR174, Next to Boarding Ground A, start 01°12.202′N, 103°52.178′E, end 01°12.141′N, 103°52.078′E, 135–79.6 m, 4 June 2013 (n = 1; DR174, ZRC.ECH.1967); sta. SUB07, SE of St. John's Island, start 01°12.671′N, 103°51.232′E, end 01°12.607′N, 103°51.145′E, 53.7–34.8 m, 19 April 2016 (n = 3; TR0316i, ZRC.ECH.1626; TR0316ii, ZRC.ECH.1627; TR0318ai, ZRC.ECH.1625); sta. SUB18,

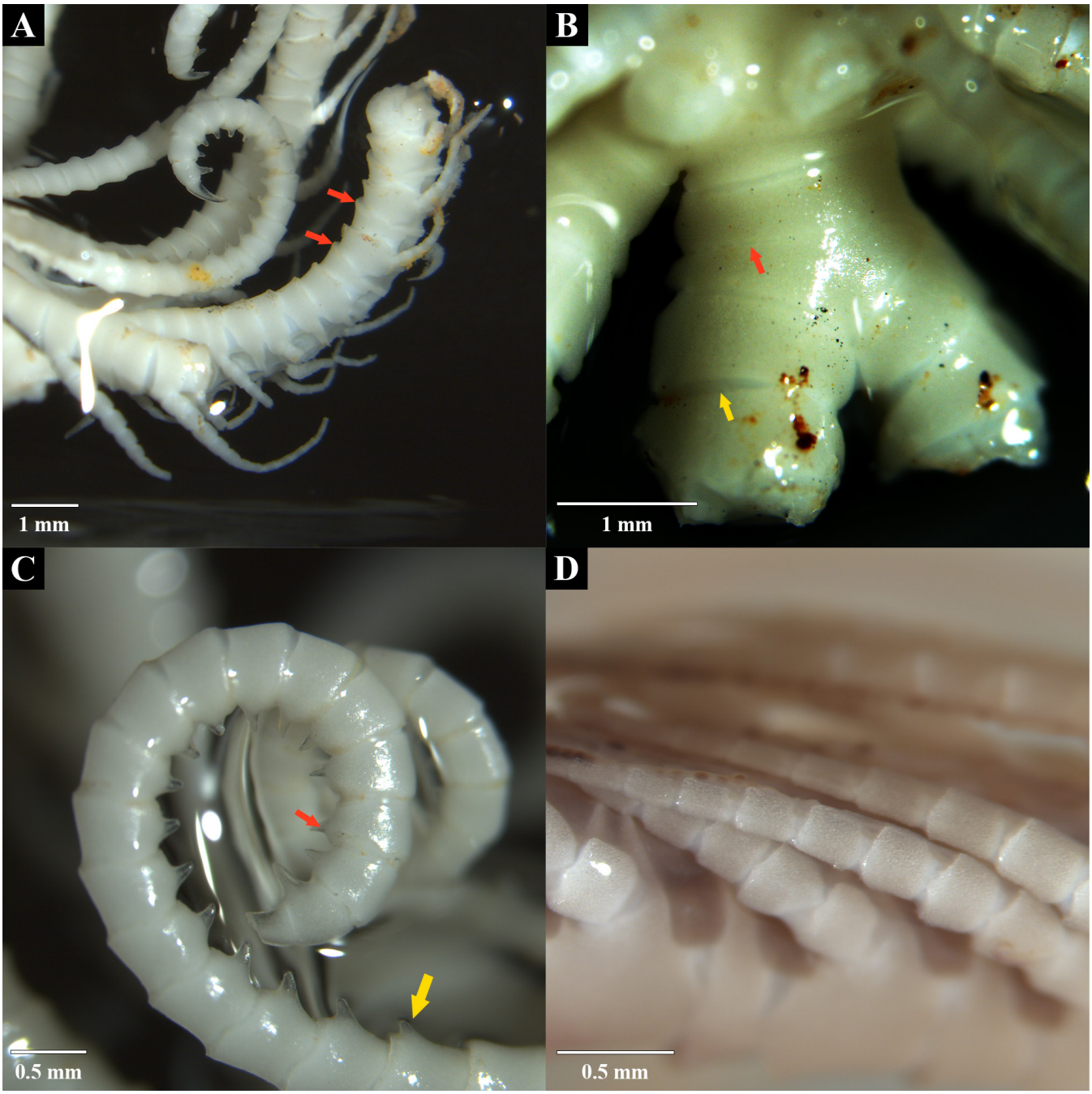

Fig. 3. *Zygometra* cf. *comata* morphological characters. A, middle brachials everted at distal margins (red arrow); B, syzygy perforation between first and second ossicles of IBr (red arrow), and synarthry (yellow arrow); C, cirri with middle to distal cirrals bearing sharp aboral spines (red arrow) that begin abruptly (yellow arrow); D, smooth and weakly carinate proximal pinnules.

SE of St. John's Island, start 01°12.682′N, 103°51.222′E, end 01°12.646′N, 103°51.135′E, 59.9–45.2 m, 2 June 2016 (n = 1; TR0966, ZRC.ECH.1634); sta. SUB36, SW of St. John's Island, start 01°12.649′N, 103°50.659′E, end 01°12.617′N, 103°50.613′E, 40.6–38.3 m, 30 June 2016 (n = 5; TR2143, ZRC.ECH.1629; TR2144i, ZRC.ECH.1678; TR2151i, ZRC.ECH.1630; TR2151ii, ZRC.ECH.1633; TR2160b, ZRC.ECH.1631).

Diagnosis. *Zygometra* with 12–35 arms in both adults and juveniles, with adult longest arm lengths between 40–135 mm but as short as 10 mm in juveniles; cirri between 15–32 cirrals, longest cirri between 28–45; first two brachials of undivided arms and proximal and distal edges of brachitaxes plain, not thickened or everted and scalloped (modified from Messing & Tay, 2016; AH Clark, 1941).

Description. Aboral surface of centrodorsal flattened and smooth; radials smooth; cirri X–XXXII (XIII and XXV in examined juvenile and adult respectively); proximal and distal cirrals broader than long; middle cirrals as broad as long; middle to distal cirrals bearing sharp, prominent aboral spine that begins abruptly (Fig. 3C). Laterally everted brachials observed on specimen (DR174, ZRC.ECH.1967), differing from the diagnosis above (Fig. 3A); specimens examined all possess IBr(1+2) (Fig. 3B) and IIBr4(3+4). Proximal pinnules generally thin and slender, and taper to a blunt point. Pinnulars smooth and weakly carinate (Fig. 3D).

Remarks. Among AH Clark's (1941) examined specimens, those from Singapore are the smallest, with 12–25 arms that are 40–70 mm long and cirri bearing 25–30 cirrals. As noted in AH Clark's (1941) monographs, *Z. comata* is variable in size-related characteristics such as the number of arms and cirrals. Given that the differences between *Z. comata* and other *Zygometra* species may be ontogenetic (Messing & Tay, 2016), the species identity of examined specimens here cannot be confidently ascertained (see Discussion). This species is distributed from the Mergui Archipelago to north-western Australia, Indonesia, Philippines, and Hong Kong (AH Clark, 1941). Depth range in Singapore 135–27 m, inhabiting substrates comprising laterite gravel, sand, reddish marine clay, or dead shells.

Family Mariametridae AH Clark, 1909d

Genus *Heterometra* AH Clark, 1909a

***Heterometra schlegelii* (AH Clark, 1908b)**
(Fig. 4)

Himerometra schlegelii AH Clark, 1908b: 223.
Amphimetra schlegelii, AH Clark, 1909a: 7.
Antedon schlegelii, AH Clark, 1909e: 117.

Holotype. ZMC CRI-41.

Material examined. Sta. DR1, Raffles Lighthouse, start 01°10.125′N, 103°45.419′E, end 01°10.211′N, 103°45.517′E, 38.5–38.3 m, 20 May 2013, (n = 1; SS-0395, ZRC.ECH.0353); sta. DR125, Sister's Island, start 01°12.416′N, 103°49.858′E, end 01°12.433′N, 103°49.817′E, 30.8–25.3 m, 30 May 2013 (n = 4; SS-3643-1, ZRC.ECH.1970; SS-3643-2, ZRC.ECH.1971; SS-3643-3, ZRC.ECH.1972; SS-3643-5, ZRC.ECH.1974); sta. SUB07, SE of St. John's Island, start 01°12.671′N, 103°51.232′E, end 01°12.607′N, 103°51.145′E, 53.7–34.8 m, 19 April 2016 (n = 8; TR0318aii, ZRC.ECH.1659; TR0320i, ZRC.ECH.1660; TR0320ii, ZRC.ECH.1661; TR0324i, ZRC.ECH.1652; TR0326ai, ZRC.ECH.1662; TR0326aii, ZRC.ECH.1653; TR0328ii, ZRC.ECH.1654; TR0328ii, ZRC.ECH.1671); sta. SUB16, SW of St. John's Island, start 01°12.646′N, 103°50.650′E, end 01°12.612′N, 103°50.495′E, 42.6–25.9 m, 27 May 2016 (n = 3; TR0657bi, ZRC.ECH.1647; TR0657bii, ZRC.ECH.1672; TR0730, ZRC.ECH.1667); sta. SUB18, SE of St. John's Island, start 01°12.682′N, 103°51.222′E, end 01°12.646′N, 103°51.135′E, 59.9–45.2 m, 2 June 2016 (n = 3; TR0971, ZRC.ECH.1651; TR0982, ZRC.ECH.1655; TR0985, ZRC.ECH.1658); SUB36, SW of St. John's Island, start 01°12.649′N, 103°50.659′E, end 01°12.617′N; 103°50.613′E, 40.6–38.3 m, 30 June 2016 (n = 18; TR2135, ZRC.ECH.1663; TR2136i, ZRC.ECH.1650; TR2136ii, ZRC.ECH.1664; TR2139, ZRC.ECH.1649; TR2144ii, ZRC.ECH.1668; TR2145, ZRC.ECH.1648; TR2146, ZRC.ECH.1673; TR2147b, ZRC.ECH.1657; TR2148ai, ZRC.ECH.1669; TR2148aii, ZRC.ECH.1646; TR2150a, ZRC.ECH.1656; TR2152, ZRC.ECH.1665; TR2154i, ZRC.ECH.1674; TR2154ii, ZRC.ECH.1670; TR2161, ZRC.ECH.1675; TR2162, ZRC.ECH.1676; TR2164i, ZRC.ECH.1666; TR2164ii, ZRC.ECH.1677); sta. TB16, Outside Eastern Boarding Ground A, start 01°13.537′N, 103°53.793′E, end 01°13.437′N, 103°53.556′E, 98–89.5 m, 21 May 2013 (n = 1; SS-0408, ZRC.ECH.0362); sta. TB28, Singapore Port Limit, start 01°13.036′N, 103°52.820′E, end 01°13.058′N, 103°52.746′E, 97.6–94.3 m, 22 May 2013 (n = 1; SS-1085, ZRC.ECH.0389); sta. TB142, Eastern Bunkering A, start 01°17.838′N, 104°04.157′E, end 01°17.851′N, 104°03.953′E, 28.8–28.7 m, 31 May 2013 (n = 1; SS-4304, ZRC.ECH.1969).

Diagnosis. IIIBr absent; distal brachials exceedingly short, discoidal; distal margins of middle brachials everted (Fig. 4A); brachials laterally flattened; cirri ~20 mm long with usually 30–35 cirrals; longest cirrals as long as broad in adults; aboral cirral spines sharp; between 10 and 14 arms (possibly up to 20), usually 70–80 mm long in adults, but can be as short as 45 mm in some adults and 16 mm in juveniles; proximal pinnules have prominent thin carinate extensions on the side towards the arm tip (Fig. 4E) (modified from Messing & Tay, 2016).

Description. Centrodorsal hemispherical to discoidal with flat aboral apex, with one juvenile having a marginal row of beads on aboral apex (SS-4304, ZRC.ECH.1969); radials beaded in juveniles, while adults show variation in smooth and beaded radials with combination of both on one specimen (SS-3643-3, ZRC.ECH.1972); cirri XV (XI–XXI in local specimens), arranged in 1–3 irregular rows; number of cirrals in local specimens 13–33; in juveniles, longest cirrals can be longer than broad, and distal cirrals possess weak carinations (Fig. 4D), triangular carinate projections (red and yellow arrows, Fig. 4C: carina broad, usually distally directed), or spines (white arrow, Fig. 4C; carina narrow, usually aborally directed); some aboral cirral spines begin as triangular carinate projections proximally but become progressively narrower and aborally directed distally (Fig. 4C); in adults, middle to distal cirrals bear distally-directed spines or blunt tubercles on aboral surface. IIBr sometimes IIBr2, mostly IIBr4(3+4); brachials plain (Fig. 4B) or everted; proximal pinnules with thin carination on basal segments, absent in one juvenile (SS-1085, ZRC.ECH.0389) (Fig. 4H); P_1 almost always shortest and most slender, except P_1 wider than P_2 in one specimen (SS-0408, ZRC.ECH.0362); distal edge of proximal pinnules sometimes ornamented with small spines on both interior and exterior lateral edges (Fig. 4G); carination at middle pinnulars in one adult specimen transitions from outer to inner ridge (Fig. 4F).

Remarks. Messing & Tay (2016) noted that Singapore specimens may have more arms, up to 19 or 20. The carinate extensions on proximal pinnules are absent on the holotype. Depth range in Singapore 103–27 m, inhabiting rocky, sandy substrates or laterite gravel.

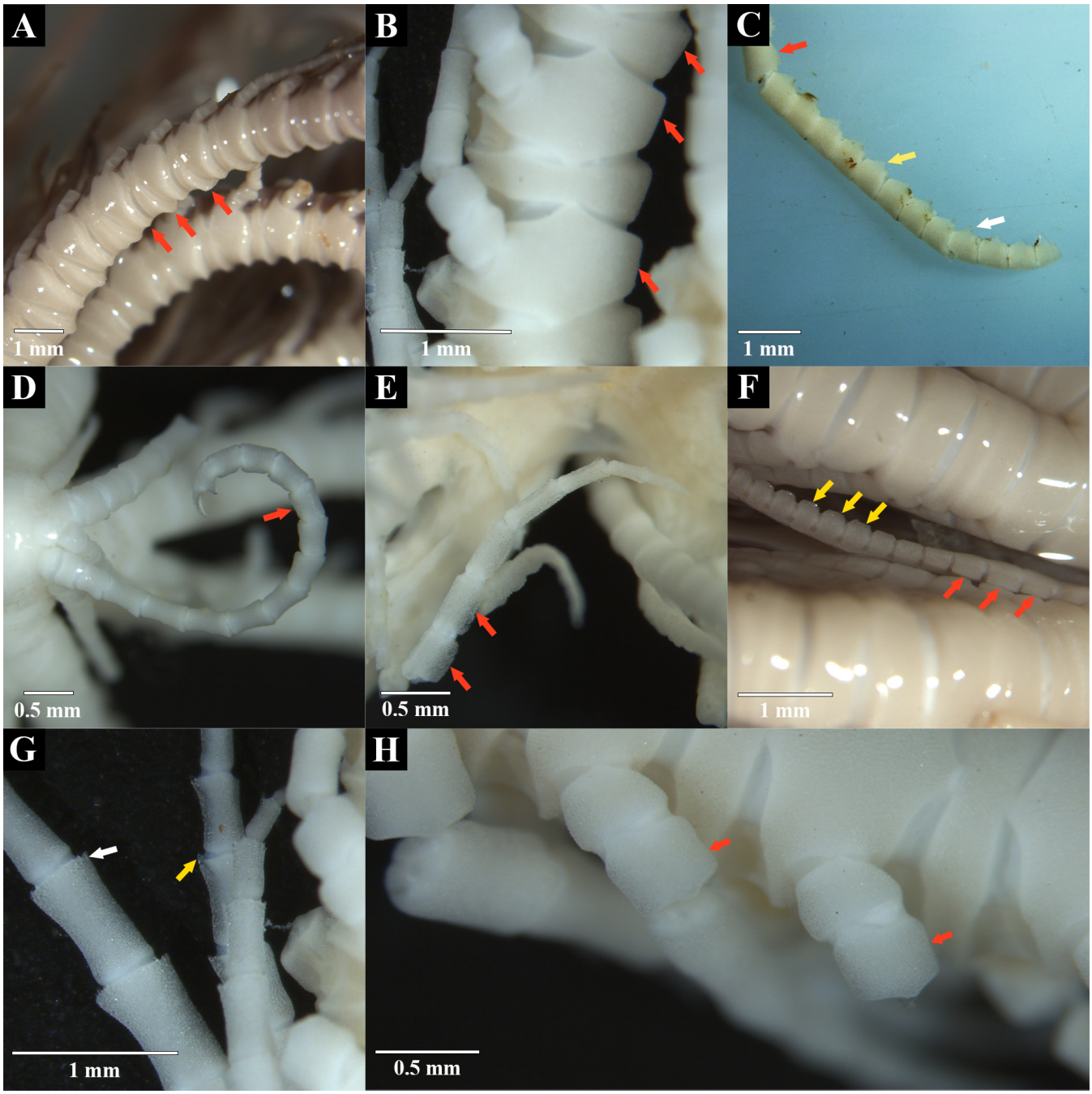

Fig. 4. *Heterometra schlegelii* morphological characters. A, distal margins of middle brachials everted in adults (red arrows); B, middle brachials of distal margins in juveniles, plain and not inverted (red arrows); C, middle cirrals of some juveniles bearing distally directed triangular projections near the distal margin of the cirral (red arrow) with projection gradually moving away from the distal edge in more distal cirrals (yellow arrow). Distal cirrals have sharp, aborally directed triangular projections or spines (white arrow); D, other juveniles have weak carinations on distal cirrals (red arrow); E, thin carinate extensions on basal segments of proximal pinnules (red arrows); F, extensions transition at middle pinnulars from facing arm tip (red arrows) to facing away from arm tip (yellow arrows) in adults; G, distal edge of distal pinnulars on proximal pinnules showing spinular side projection (yellow arrow) and premature rim of serration (white arrow); H, basal segments of proximal pinnules of one juvenile (SS-1085, ZRC.ECH.0389) bearing very weak carinate extensions on basal segments.

Genus *Dichrometra* AH Clark, 1909a

***Dichrometra* sp.**
(Fig. 5)

Material examined. Sta. DR111, Outside Eastern Boarding Ground A, start 01°12.989′N, 103°53.062′E, end 01°12.862′N, 103°52.852′E, 136–125 m, 29 May 2013 (n = 1; SS-3634, ZRC.ECH.1968); sta. DR125, Sister's Island, start 01°12.416′N, 103°49.858′E, end 01°12.433′N, 103°49.817′E, 30.8–25.3 m, 30 May 2013 (n = 1; SS-3643-4, ZRC.ECH.1973); sta. TB28, Singapore Port Limit, start 01°13.036′N, 103°52.820′E, end 01°13.058′N, 103°52.746′E, 97.6–94.3 m, 22 May 2013 (n = 1; SS-0967, ZRC.ECH.0371); sta. TB96, Eastern Bunkering A, start 01°18.140′N, 104°04.22′E, end 01°18.329′N, 104°04.396′E, 25.1–22.4 m, 28 May 2013 (n = 4; SS-2538-1, SS-2538-2, SS-2538-3, SS-2538-4, ZRC.ECH.0442).

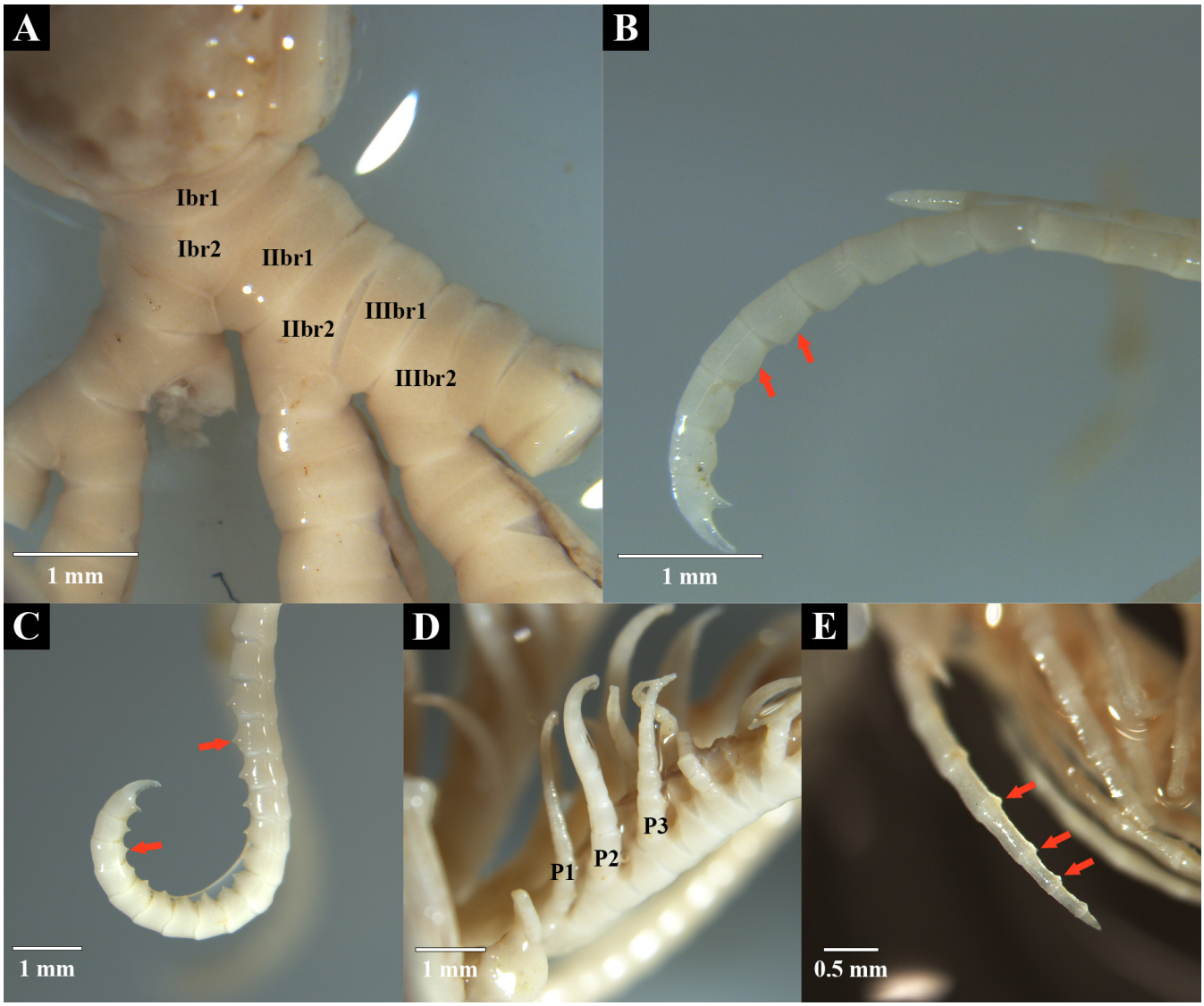

Fig. 5. *Dichrometra* sp. morphological characters. A, division series illustrating two ossicles each of IBr2 (IBr1–IBr2), IIBr2 (IIBr1–IIBr2) and IIIBr2 (IIIBr1–IIIIBr2) division series; B, cirri with distal cirrals aborally carinate (red arrow); C, cirri with middle to distal cirrals bearing sharp aboral spines (red arrow); D, proximal pinnules distally flagellate and tapering to a point. P2 longer and basally stouter than P1 and P3; E, spinular side projection on distal edge of distal pinnulars on proximal pinnules on one juvenile (SS-2538-2, ZRC.ECH.0442).

Diagnosis. *Dichrometra* with P_2 the longest or stoutest (Fig. 5D); cirri XI–XXIV, slender, or short and stout, with 13–28 cirrals; basal cirrals always broader than long; middle to distal cirrals aborally carinate (Fig. 5B), spinose (Fig. 5C), or each bearing a distally-directed triangular projection; brachials on undivided arm plain; between 10–30 arms; IIBr either consists of 2 ossicles or 4(3+4) (Fig. 5A); proximal pinnules generally thin and slender, but can possess spinular side projection (Fig. 5E) or carinations on distal edge of distal pinnulars in juveniles.

Description. Centrodorsal hemispherical to discoidal; basal diameter from 0.75 to 2.56 mm in juveniles, to 3.45 mm in adults; aboral pole flat or convex, smooth with no granulation, although bead-like tubercles observed on four juveniles. Cirri XIII–XVIII, 13–28 cirrals in juveniles; cirral ornamentation variable, with middle to distal cirrals aborally carinate, or possessing spines or triangular projections; on one specimen, middle cirrals bearing blunt spines progress into sharper spines on distal cirrals (SS-2538-3, ZRC.ECH.0442). Brachitaxes mostly of two ossicles joined by synarthry (Fig. 5A); two juvenile specimens with IIBr4(3+4) observed; brachials on undivided arm aborally plain; proximal pinnules distally flagellate and tapered to a point with no projection in the adult specimen, but variable in juveniles; smooth with no projections, or possess small spines on distal edges.

Remarks. This species is clearly distinguished from all other *Dichrometra* spp. based on the phylogeny obtained. Nevertheless, it resembles *D. palmata* in its superior size of P_2 (Taylor et al., 2018), ranging from 1.07 mm to 4.33 mm in length and 0.1 to 0.36 mm in width (with the exception of SS-2538-1, ZRC.ECH.0442, which has P_3 as the longest and stoutest pinnule). The size range of P_2 in *D. palmata* is not known. *Dichrometra palmata* possesses distally flagellate proximal pinnules, and its distal cirrals are usually aborally carinate, occasionally with a spine (Messing & Tay, 2016; Taylor et al., 2018). This species has distal projections on proximal pinnules and variable cirral ornamentation (see above). Adult descriptions may be subject to further

clarification as only one adult specimen was examined in the study. Furthermore, given that the type material of species synonymised with *D. palmata* in AH Clark (1941) are unexamined, and the uncertainty of proximal pinnule relative sizes as diagnostic characters, this species cannot be confidently placed in *D. palmata*. Depth range in Singapore 136–22 m, inhabiting substrates comprising clay, laterite gravel, or sand. Myzostomid worm observed on one specimen (SS-2538-3, ZRC.ECH.0442).

DISCUSSION

This study assesses whether current taxonomic descriptions contain sufficient information for identifying himerometroid crinoids from Singapore, including juvenile specimens. The species identity of specimens identified as *Heterometra* cf. *producta* is also tested. Based on the molecular phylogeny reconstruction using partial sequences of COI, the identities of most examined specimens are incongruent at the genus level, highlighting limitations of currently accepted diagnostic features based solely on adult specimens. Additionally, the analysis of specimens originally identified as *He.* cf. *producta* attributes misidentification to shared morphological characters that are diagnostic for *He. producta*, bringing into question the validity of this species.

With the exception of *Heterometra*, genera under the family Mariametridae, including *Dichrometra*, can be identified by brachitaxes only comprising of two ossicles joined by synarthry. Currently, *Dichrometra* is characterised by P_2, or P_2 and P_3 being longer and larger than P_1 as well as distally flagellate proximal pinnules, and *D. palmata* is distinguished from other *Dichrometra* species by their P_2 which is "substantially longer and stouter basally than both P_1 and P_3" (Taylor et al., 2018). While all the examined specimens possess the family- and genus-level diagnostic features, P_2 is not the tallest or basally stoutest proximal pinnule in one juvenile specimen (centrodorsal diameter, or cd = 1.4–1.72 mm). Furthermore, other size-related diagnoses such as the number of arms and pinnulars do not apply to juveniles as they can have as few as 10 arms (cf. 20–30 in adult) and less than 10 pinnulars (cf. 17–26 in adult) on each proximal pinnule. This shows that these diagnostic characters are indeed subjected to ontogenetic variation and, thus, the use of such characters for juvenile identification is limited. Clearly, molecular data are necessary to determine the species identities of these *Dichrometra* juveniles.

With the high nodal support in the molecular phylogeny (Fig. 1), seven specimens form a reciprocally monophyletic clade with the rest of *Dichrometra* despite their morphological similarities with *Dichrometra palmata*. The distally flagellate proximal pinnules and relative sizes of proximal pinnules may therefore be limited in their usefulness as diagnostic characters. Furthermore, *D. palmata* has been noted to be widely variable in the structure of their proximal pinnules and cirri (AH Clark, 1941; Taylor et al., 2018). Taylor et al. (2018), for example, observed that some cirri had aboral spines while others only bore carinations, and proximal pinnule sizes also ranged between $P_1 < P_3$, and $P_1 > P_3$. Due to uncertainties in the morphological diagnosis and phylogenetic position of these specimens, they are herein treated as *Dichrometra* sp.

Among the seven *Dichrometra* sp. specimens, six juveniles were initially identified as *Heterometra* species, and one adult was assigned to *He.* cf. *producta* (discussed below). The misidentification could be attributed to the premature state of the diagnostic characters in juvenile specimens as well as the highly variable nature of *Heterometra*'s diagnostic features. In particular, one juvenile specimen has spinular side projections on the distal edge of pinnulars of proximal pinnules, while the remaining two possess smooth pinnulars without projections on proximal pinnules. The different proximal pinnular ornamentation between the specimens might have been mistaken for *Heterometra* because members of the genus were reported to feature pinnulars that are "smooth, carinate or distally spinose, or flanged" (Messing & Tay, 2016). Furthermore, another diagnostic character of *Heterometra* concerns the two or four ossicles in the brachitaxes (Hess & Messing, 2011). Since the division series of all juveniles have two ossicles, they could be erroneously recognised as *Heterometra* as well.

The *He. schlegelii* specimens in this study have been placed in the same *Heterometra* clade as in Foo et al. (2021), sister to *Amphimetra* spp. within Mariametridae (Fig. 1). This is highly supported, although two specimens possess IIBr2; the rest have IIBr4(3+4), which deviates from the family-level diagnosis. However, across most examined specimens, proximal pinnules have diagnostic characters of the species: thin, carinate extensions are present on the basal segments of enlarged proximal pinnules (Hess & Messing, 2011). Only one juvenile (SS-1085, ZRC.ECH.0389; cd = 2 mm; arm length = 33 mm) displayed an immature form of this feature, bearing very weak carinate extensions on basal segments (Fig. 2H). On one adult specimen (SS-3643-5, ZRC.ECH.1974; cd = 2.56, arm length = 61 mm), the transition of carinated extensions at the sixth or seventh pinnular from the side towards arm tip to away from arm tip can be observed, consistent with Foo et al. (2021). IIIBr is also absent in all specimens, but as shown in Foo et al. (2021), this trait may not be a useful diagnostic character, because IIIBr may also be absent in other species depending on their developmental stage.

Of the eight *He. schlegelii* specimens, four were originally identified as *He.* cf. *producta* (see below) and one as *Ho*. cf. *crenulata*. For the latter, misidentification could be due to the sharp side projection on the distal edge of distal pinnulars on proximal pinnules on some juveniles (Fig. 4G) which may be perceived as an immature precursor to spinose projections on *Ho.* cf. *crenulata* (Messing & Tay, 2016). However, other distinguishing characters including the distal portion of prismatic ridges being raised into broad rounded triangular processes were not observed in the specimens (Messing & Tay, 2016). The thin carinate extensions on basal segments of proximal pinnules therefore remain as the most reliable diagnostic character for *He. schlegelii* in adults, but this

requires further examination in juveniles which may display an immature form of the feature.

The perfect syzygy on IBr2(1+2) in *Zygometra* (AH Clark, 1941) is its most distinguishable character, even in juveniles. Our molecular phylogeny places the single *Zygometra* specimen in this study within the same clade as *Z.* cf. *comata* of Foo et al. (2021) and sister to *Z. andromeda*, with high ML support. While the specimens have brachials with everted distal ends, unlike the diagnostic plain brachials of *Z.* cf. *comata* (Messing & Tay, 2016), they are not tuberculated or scalloped, which are diagnostic for *Z. andromeda*. Furthermore, intraspecific genetic distances within *Z.* cf. *comata* are much lower than interspecific distances with *Z. andromeda*. Foo et al. (2021) observed that *Z.* cf. *comata* possesses a rim of serration on the distal edge of pinnulars on proximal pinnules, but this character is not seen in the specimens of this study. Instead, its proximal pinnules are slender, weakly carinated, and taper to a point, which matches the diagnosis of *Z. comata* in AH Clark (1941). This confusion between *Zygometra* spp. is not surprising, since "five out of six *Zygometra* species are largely distinguished based on size-related meristic characters" (Messing & Tay, 2016: 654), and three out of the five have intermediate forms that exist between them, as AH Clark (1941) had noted. It is therefore hypothesised that the differences between *Z. comata* and other *Zygometra* specimens could be ontogenetic (Messing & Tay, 2016). Furthermore, another *Z. comata* (FMNH-13295) is not sister to our *Z.* cf. *comata* terminals, so we suggest that *Zygometra* may be monospecific based on overlapping morphological characters and phylogenetic branch lengths constructed using COI (Foo et al., 2021). Further clarification, supported by additional genetic sequences and observations of *Z. andromeda*, is needed to assess the status of *Zygometra comata*.

Morphological examination and molecular phylogeny inference have resulted in the combination *Homalometra crenulata* proposed by Foo et al. (2021). Currently, the diagnosis for the *Homalometra* genus includes having 10 or 11 arms, and slender cirri tapering to a point (AH Clark, 1941). However, Foo et al. (2021) observed that specimens they examined and the holotype display deviations from this diagnosis, with some cirri on the holotype bearing a weak opposing spine, while some Singapore specimens have a combination of both characters on different cirri. This variation warrants a revision in the diagnosis of the *Homalometra* genus as its usefulness is limited in its current state, especially when it needs to be distinguished from *Heterometra* species. Additionally, juvenile features also differ from adults of this species, in particular the absence of carination on proximal pinnulars of proximal pinnules, and the absence of bead-like tubercles on the distal edges of radials on one juvenile specimen. These ontogenetic differences exacerbate the confusion between *Ho. crenulata* and *Heterometra* as these characters are also present in *Heterometra* species such as *He. schlegelii*. Including these exceptions in the revised description would help to clarify boundaries concerning these variable juvenile characters between *Ho. crenulata* and other adult *Heterometra* specimens.

All specimens originally identified as *He.* cf. *producta* (n = 7) bear the diagnostic character of *He. producta*—smooth proximal pinnules with no projection (AH Clark, 1941)—but they have returned as three distinct species (*Zygometra* cf. *comata*, *Heterometra schlegelii*, and *Dichrometra* sp.) on the phylogenetic tree (Fig. 1). These specimens also share common cirri ornamentation, bearing uniform triangular spines pointing distally that range from blunt to sharp, although this is not diagnostic of the species. The confusion of these specimens with *He.* cf. *producta* suggests that this particular proximal pinnules ornamentation may not be informative taxonomically and thus ought to be used with caution in family- and genus-level diagnoses. This result agrees with AH Clark's (1941) observations of *He.* cf. *producta* being similar to other *Heterometra* species and puts the validity of *He.* cf. *producta* as a species into question, as it may be conspecific with *He. propinqua* or even *Ho. crenulata*. Given that *He. producta* was described from only four specimens (AH Clark, 1941), further study of *He.* cf. *producta* is warranted to clarify the species status.

In conclusion, this study shows that juvenile Himerometroidea specimens cannot be confidently identified based on morphology due to overlapping traits between different taxa and the immature state of some characters. Therefore, we have expanded the existing taxonomic descriptions of *Zygometra* cf. *comata*, *Heterometra schlegelii*, and *Dichrometra* sp. to include variations in juvenile morphology, and discussed lapses in diagnostic characters of *Heterometra* spp. when compared with other species. We have also redescribed *Homalometra crenulata* based on Singapore specimens studied by Foo et al. (2021). Overall, our findings here highlight the challenges of solely using morphological data to determine species-level identities, and emphasise the need for integrating molecular data with morphological observations to revise diagnostic characters of specific crinoid genera and families.

ACKNOWLEDGEMENTS

This research is supported by the Lee Kong Chian Natural History Museum, National University of Singapore. We are grateful to contributors of the Comprehensive Marine Biodiversity Survey—jointly led by the National Parks Board and National University of Singapore—that provided the material for this study. We thank David L. Meyer, Koh Siang Tan, and two anonymous reviewers for constructive comments.

LITERATURE CITED

Baumiller TK, Salamon MA, Gorzelak P, Mooi R, Messing CG & Gahn FJ (2010) Post-Paleozoic crinoid radiation in response to benthic predation preceded the Mesozoic marine revolution. Proceedings of the National Academy of Sciences of the United States of America, 107: 5893–5896.

Bell FJ (1882) An attempt to apply a method for formulation to the species of the Comatulidae; with a description of a new species. Proceedings of the Zoological Society of London, 6: 530–536.

Carpenter PH (1882) Description of new or little known Comatulae. I. On the species of *Atelecrinus* and *Eudiocrinus*. II. The Comatulae of the Hamburg Museum. Journal of the Linnean Society of London (Zoology), 16: 487–526.

Carpenter PH (1888) Report on the Crinoidea collected during the voyage of H.M.S. Challenger, during the years 1873-76. Part II. The Comatulae. Reports of the Scientific Results of the Voyage of H.M.S. Challenger, Zoology, 26 (part 60): 1–402, pls. 1–70.

Clark AH (1907) New genera of recent free crinoids. Smithsonian Miscellaneous Collections, 50: 343–364.

Clark AH (1908a) Descriptions of new species of crinoids, chiefly from the collections made by the U.S. Fisheries steamer "Albatross" at the Hawaiian Islands in 1902; with remarks on the classification of the Comatulida. Proceedings of the United States National Museum, 34: 209–239.

Clark AH (1908b) New genera and species of crinoids. Proceedings of the Biological Society of Washington, 21: 219–232.

Clark AH (1908c) New genera of unstalked crinoids. Proceedings of the Biological Society of Washington, 21: 125–136.

Clark AH (1909a) A revision of the crinoid families Thalassometridae and Himerometridae. Proceedings of the Biological Society of Washington, 22: 1–22.

Clark AH (1909b) Descriptions of seventeen new species of Recent crinoids. Proceedings of the United States National Museum, 36: 633–651.

Clark AH (1909c) Five new species of recent unstalked crinoids. Proceedings of the United States National Museum, 37: 29–34.

Clark AH (1909d) New genera and higher groups of unstalked crinoids. Proceedings of the Biological Society of Washington, 22: 173–178.

Clark AH (1909e) On a collection of crinoids from the Copenhagen Museum. Videnskabelige Meddelelser fra den naturhistoriske Forening i Kjöbenhavn, 1909: 115–194.

Clark AH (1911) The recent crinoids of Australia. Memoirs of the Australian Museum, 4: 705–804.

Clark AH (1912) The Crinoids of the Indian Ocean. Echinoderma of the Indian Museum, Part VII. Indian Museum, Calcutta, 325 pp.

Clark AH (1913) The crinoids of the Natural History Museum at Hamburg. Smithsonian Miscellaneous Collections, 60: 1–33.

Clark AH (1915) A monograph of the existing crinoids. Volume 1. Part 1. Bulletin of the United States National Museum, 82: 1–406, 17 pls.

Clark AH (1918) The unstalked crinoids of the Siboga Expedition. Siboga–Expeditie, 42b: 1–300, 28 pls.

Clark AH (1921) A monograph of the existing crinoids 1(2). Bulletin of the United States National Museum, 82: 1–795, 57 pls.

Clark AH (1929) On some recent crinoids in the collection of the British Museum. Zoological Journal of the Linnean Society of London, 36: 635–664.

Clark AH (1931) A monograph of the existing crinoids 1(3). Bulletin of the United States National Museum, 82: 1–916, 82 pls.

Clark AH (1941) A monograph of the existing crinoids 1(4a). Bulletin of the United States National Museum, 82: 1–603, 61 pls.

Clark AH (1947) A monograph of the existing crinoids 1(4b). Bulletin of the United States National Museum, 82: 1–473, 43 pls.

Clark AH (1950) A monograph of the existing crinoids 1(4c). Bulletin of the United States National Museum, 82: 1–383, 32 pls.

Clark AH & Clark AM (1967) A monograph of the existing crinoids 1(5). Bulletin of the United States National Museum, 82: 1–860.

Folmer O, Black M, Hoeh WR, Lutz R & Vrijenhoek RC (1994) DNA primers for amplification of mitochondrial cytochrome c oxidase subunit I from diverse metazoan invertebrates. Molecular Marine Biology and Biotechnology, 3: 294–299

Foo SH, Taylor KH, Messing CG, Rouse GW, Tay TS, Tan KS & Huang D (2021) Assessing the taxonomy of *Heterometra*-like feather stars (Echinodermata: Crinoidea: Himerometroidea) based on morphology and molecular data. Systematics and Biodiversity, 19: 632–647.

Helgen LE & Rouse GW (2006) Species delimitation and distribution in *Aporometra* (Crinoidea: Echinodermata): endemic Australian featherstars. Invertebrate Systematics, 20: 395–414.

Hemery LG, Roux M, Améziane N & Eleaume M (2013) High-resolution crinoid phyletic inter-relationships derived from molecular data. Cahiers de Biologie Marine, 54: 511–523.

Hess H (1999) Permian. In: Hess H, Ausich WI, Brett CE & Simms MJ (eds.) Fossil crinoids. Cambridge University Press, Cambridge, pp. 160–163.

Hess H & Messing C (2011) Treatise on Invertebrate Paleontology, Part T, Echinodermata 2 (Revised) Vol. 3: Crinoidea. University of Kansas and Paleontological Institute, Lawrence, 261 pp.

Huelsenbeck JP & Ronquist F (2001) MRBAYES: Bayesian inference of phylogenetic trees. Bioinformatics, 17: 754–755.

Katoh K, Misawa K, Kuma K & Miyata T (2002) MAFFT: a novel method for rapid multiple sequence alignment based on fast Fourier transform. Nucleic Acids Research, 30: 3059–3066.

Katoh K & Standley DM (2013) MAFFT multiple sequence alignment software version 7: improvements in performance and usability. Molecular Biology and Evolution, 30: 772–780.

Kearse M, Moir R, Wilson A, Stones-Havas S, Cheung M, Sturrock S, Buxton S, Cooper A, Markowitz S, Duran C, Thierer T, Ashton B, Meintjes P & Drummond A (2012) Geneious Basic: An integrated and extendable desktop software platform for the organization and analysis of sequence data. Bioinformatics, 28: 1647–1649.

Leray M, Yang JY, Meyer CP, Mills SC, Agudelo N, Ranwez V, Boehm JT & Machida RJ (2013) A new versatile primer set targeting a short fragment of the mitochondrial COI region for metabarcoding metazoan diversity: application for characterizing coral reef fish gut contents. Frontiers in Zoology, 10: 34.

Messing CG & Tay TS (2016) Extant Crinoidea (Echinodermata) of Singapore. Raffles Bulletin of Zoology, Supplement 34: 627–658.

Müller J (1841) Über die Gattungen und Arten der Comatulen. Monatsberichte Königlich Preussische Akademie der Wissenschaften zu Berlin, 1841: 179–189 (also Archiv für Naturgeschichte, 7: 139–148).

O'Hara TD, Hugall AF, Thuy B & Moussalli A (2014) Phylogenomic resolution of the Class Ophiuroidea unlocks a global microfossil record. Current Biology, 24: 1874–1879.

Owen CL, Messing CG, Rouse GW & Shivji MS (2009) Using a combined approach to explain the morphological and ecological diversity in *Phanogenia gracilis* Hartlaub, 1893 (Echinodermata: Crinoidea) *sensu lato*: two species or intraspecific variation? Marine Biology, 156: 1517–1529.

Posada D (2008) jModelTest: phylogenetic model averaging. Molecular Biology and Evolution, 25: 1253–1256.

Reichensperger A (1913) Ungestielte crinoideen der Aru- und Kei-Inseln. Abhandlungen der Senckenbergischen Naturforschenden Gesellschaft, 35: 79–108.

Ronquist F, Teslenko M, Mark P van der, Ayres DL, Darling A, Höhna S, Larget B, Liu L, Suchard MA & Huelsenbeck JP (2012) MrBayes 3.2: Efficient Bayesian phylogenetic inference and model choice across a large model space. Systematic Biology, 61: 539–542.

Stamatakis A (2006) RAxML-VI-HPC: Maximum likelihood-based phylogenetic analyses with thousands of taxa and mixed models. Bioinformatics, 22: 2688–2690.

Stamatakis A (2014) RAxML version 8: a tool for phylogenetic analysis and post-analysis of large phylogenies. Bioinformatics, 30: 1312–1313.

Summers MM, Messing CG & Rouse GW (2014) Phylogeny of Comatulidae (Echinodermata: Crinoidea: Comatulida): A new classification and an assessment of morphological characters for crinoid taxonomy. Molecular Phylogenetics and Evolution, 80: 319–339.

Summers MM, Messing CG & Rouse GW (2017) The genera and species of Comatulidae (Comatulida: Crinoidea): taxonomic revisions and a molecular and morphological guide. Zootaxa, 4268: 151–190.

Tan KS, Koh KS, Ng JY & Goh L (2016) The Comprehensive Marine Biodiversity Survey Singapore Strait International Workshop 2013. Raffles Bulletin of Zoology, Supplement 34: 1–7.

Taylor KH (2015) A phylogenetic revision of superfamily Himerometroidea (Echinodermata: Crinoidea). Unpublished PhD Thesis. Nova Southeastern University, Fort Lauderdale, 170 pp.

Taylor KH, Rouse GW & Messing CG (2017) Systematics of *Himerometra* (Echinodermata: Crinoidea: Himerometridae) based on morphology and molecular data. Zoological Journal of the Linnean Society, 181: 342–356.

Taylor KH, Rouse GW & Messing CG (2018) Revising Mariametridae: the genera *Dichrometra*, *Lamprometra*, and *Liparometra* (Echinodermata: Crinoidea). Systematics and Biodiversity, 16: 142–159.